Comparative Study of CaF and CaO, and Elemental Analysis of Fluorite Gemstone by Calibration Free Laser Induced Breakdown Spectroscopy

Muhammad Raza[1], Muhammad Sharif [2]

[1]Department of Physics, Karakoram International University, Gilgit, Gilgit-Baltistan, Pakistan
[2]Government High School Dambudas Roundu, Skardu, Baltistan, Pakistan

Abstract: Laser-induced breakdown spectroscopy is the most intellectual and best technique that contributes well to mineralogy for qualitative and quantitative chemical analysis using the Origi Software 9.1 version. In this study, by using CL-LIBS, we calculated Ca 88%, iron 9%, Si, and Na 1 % respectively, in the Fluorite gemstone. Fluorite is used in decorative pieces and jewelry just because of the major concentration of Ca, and less detected molecules mentioned as CaO and CaF are secreted in Fluorite Gemstones. It was the first time anyone had worked on such minerals. The determination of elemental composition, major and trace elements, and the fingerprint of Greenish-Fluorite gemstone was carried out in this study. This Greenish-Fluorite gemstone was collected from Astak mine, Rondo Valley, Gilgit-Baltistan, Pakistan. The highest peaks of Ca-I are observed at 585.74 nm, lithium at 760.77 nm, and sodium at 588.99nm. The observed spectra line shows CaF found at a range of 590 - 608 nm, and CaO at 616 - 625 nm.

Keywords: Fluorite, CL-LIBS, Quantification, Astak Mine, Gilgit-Baltistan.
Email: raza.physics@kiu.edu.pk

1. Introduction

Laser induce breakdown spectroscopy (LIBS) is emerge as powerful versatile and strong analytical tools [1], which is a unique, fast, remote, and sensitive technique and no needs of samples formation [2] for determination of quantitative and qualitative analysis of elemental composition of all kind of samples solid, liquid, and gases [3] since last few year it's also used to determine the elemental composition of alloys, metal alloys, oxide, Nano-structure, aerology, meteorites, rock [4, 5] gemstones etc. The calibration-free laser-induced breakdown spectroscopy (CF-LIBS) may also be used for jewelry appraisal, archeological, and geological analysis gives the emission or absorption spectrum line of all kinds of samples based on the chemical and physical properties of samples, especially surface properties [6, 7]. Calibration-free LIBS, Csigma LIBS, one-point multi-line calibration free LIBS (OP-MLC-LIBS), and single sample calibration LIBS (SSC-LIBS) require a matrix-match stander and comparison [8], because of its unique, fast, economical method. LIBS is used in biological fields such as teeth, bone, [9] leaf, and blood, as well as environmental applications [10].

In LIBS, high-intensity lasers laser focused on the surface of samples, which produces a plasma plume on the surface of samples [11], which cools down within an instant time interval and emits different spectral lines based on composition. These emission spectra give different calibration curves that represent the chemical composition of Fluorite samples [12]. There are multiple methods that are applicable to calculate the major and trace elements of fluorite gems, inductively coupled plasma mass spectroscopy (ICP-MS) [13], inductively coupled plasma optical emission (ICP-OES), and atomic absorption spectroscopy (AAS) [14]. Wherever the Limits of Detection (LOD) are gradually higher than conventional methods [15, 16].

1.1 About Fluorite Gemstone

Fluorite gemstones consist of fluorite, also known as fluorspar in which calcium fluoride, belong to halide having crystallizes in, isometric cube motif, octahedral, and more complex features. It is a precious, unique, and adorable gemstone found in various countries, and originated in Gilgit-Baltistan, particularly in Roundu, Shigar [17], and Nagar Valley. Fluorite is derived from the Latin verb fluere (meaning to flow). Fluorite has four perfect cleavage planes that help to produce octahedral fragments, and the most common one is the motif adopted by fluorite.

Nigeria is known as the basecamp of Fluorite gems, with another precious gemstone. The fluorite gemstone is found in various colors such as white, yellow, green, blue, yellowish, greenish, colorless, and purple [18]. Fluorite gemstones are transparent to translucent minerals of CaF and CaO [5], an isomeric system [19] mostly found in crystalline or large cubic crystal shapes with whitish or faintly colored one or more cleavages, purple, green, blue [20], yellow, violet-blue, sky-blue, green, [21] brown, and many more [22]. The softness is 4 Mohs, while the hardness is less than 5.5 Mohs [23] Crystal class of Fluorite is hex-octahedral, with unit cell a = 5.4626 A°. The specific gravity is in the range of 3.15 - 3.184 to 3.56. It is highly rare earth elements with a reflective index of 1.433 - 1.448. Solid fluorite is also used for electrolytes and electrochemical processes. Calcium fluoride (CaF) by laser-induced breakdown spectroscopy (LIBS), and also obtain quantitative fluoride distribution images of teeth. LIBS has proved to be an efficient technique to detect low amounts of fluoride in solids, and human teeth have the advantage of being a matrix rich in calcium [24]. The general properties are given in Table 01.

Table 01 Properties of Fluorite

Sample	IMA symbol	Crystal system	Crystal class	Color	Mohs scale	Specific gravity	Refractive index
Fluorite gemstone	Flr	Isometric	Hex-Octahedral	Colorless, purple, lilac, golden-yellow, green, blue, pink, brown	4 hardness	3.175 - 3.184	1.433 - 1.448

2. Experimental Setups

The scheme diagram of laser-induced breakdown spectroscopy is given in Fig.01. A sample of Fluorite Gemstone from the mining area of Astak Roundu. The sample was 5 mm thick with a 1.5 cm diameter. The Q-switched Nd: YAG laser of first harmonic, having the wavelength in the range of 1046 nm and the second harmonic laser 532 nm, capable of delivering 500 mJ pulse energy, 5 ns pulse duration, and 10 Hz repetition rate, was used for the LIBS, having the energy 110 mJ for an interval of 2 µs. A sample placed focused from 10 cm with a high-intensity laser, producing the plasma plume on the surface of the samples to produce the emission and absorption spectral lines from the surface of the samples [3, 25]. The absorption spectral line was extracted with the help of software called Origin 9.1, which compares to the extracted data found in the NIST database (https://www.nist.gov/pml/), which can generate absorption wave data from 220 nm to 900 nm [6,13].

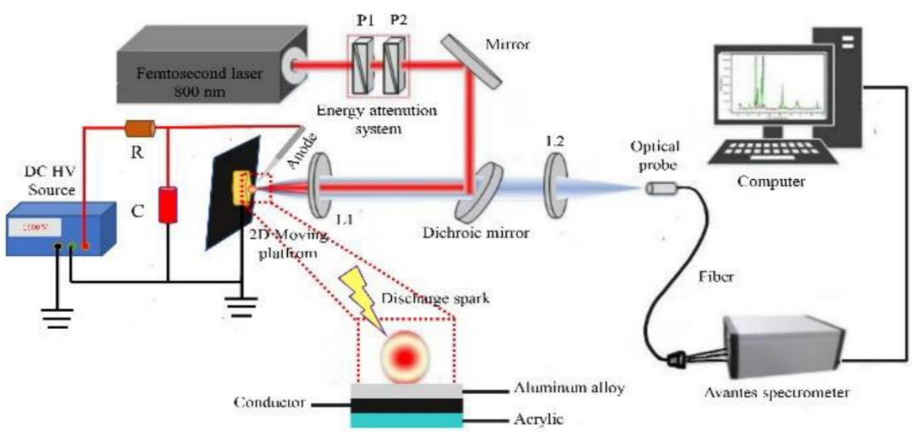

Figure 01 Scheme Diagram of CL-LIBS

3. Methodology of CF-LIBS

LIBS is used to determine the composition of elements present in samples. Calcium, Sodium, Potassium, Silicon, Iron, Magnesium, Aluminum, Titanium, Lead, Manganese, Sodium Carbon are found in different concentrations in different samples. Nd: YAG laser has a pulse energy of ~130 mJ and second harmonic with wavelength of 532 nm, is used for spectral analysis, which is recorded by using a spectrometer for both the qualitative and quantitative analysis of collected samples from Astak mine, Roundu.

3.1 Atomic Emission Spectrometry Based on Plasma Sources

Plasma is the combination of an aggregate of a huge concentration of electrons and cations. Electrical conductors can heat inductively with the aid of coupling and oscillating magnetic discipline. The plasma temperature is in the order of 6,000 K to 9,000 K. Primarily, plasma is based on AES in principle, which is like flame photometry, and the simplest distinction being of flame is replaced by a good deal more active atomization-excitation methods of plasma. The employment of plasma is argon with emission radiation. This emission intensity from different stones for ionized lines has different patterns, with plenty having higher peaks as compared to corresponding neutral emission lines intensities. The different tender patterns contain the same elements due to the lower plasma amplification of velocity, due to the weak repulsive force supplied via the soft goal. Therefore, emission intensity ratios between neutral line and ionic line are used to estimate the pattern hardness of samples [26]. As discussed above that the spectral line has a range of 220 nm – 900 nm, and the tentative graph is discussed below in detail.

4. Results

The emission spectral line obtained from the Q-switch Nd-GAY laser second harmonic graph was compared with the NIST database one by one, as follows:

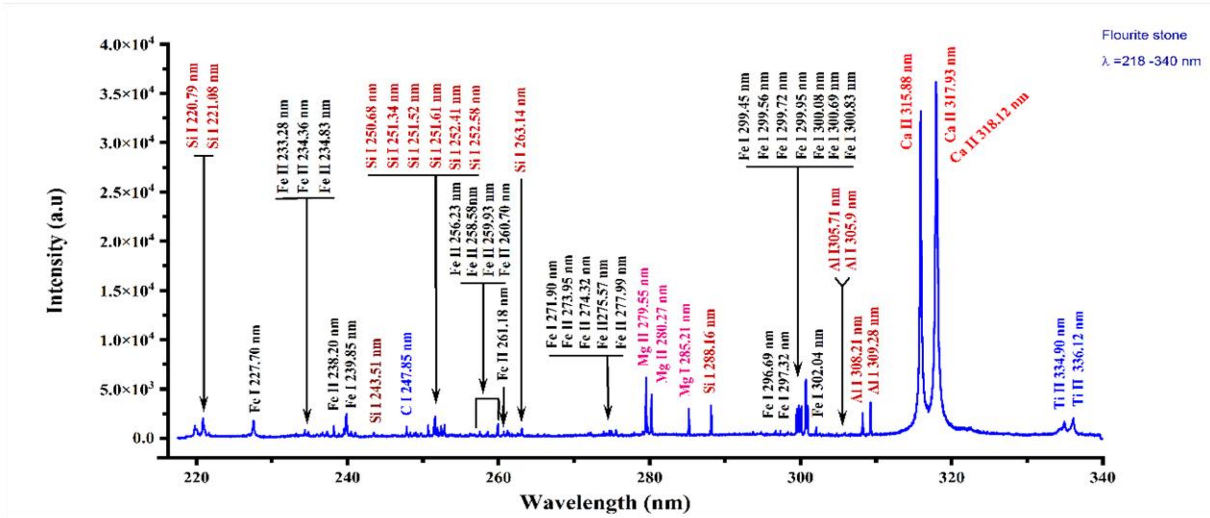

Figure 02. Optical emission spectrum of the Fluorite sample representing the spectral line of all the identified elements exists in the range of 220 nm – 340 nm.

The spectrum is about the sample of fluorite gemstone in the range of 220 nm to 340 nm collected from Astak mine, Roundu, Gilgit-Baltistan, Pakistan. The neutral and ionized spectrums found in the figure given express the major and trace elements. The highest peaks of neutral silicon are at 288.21 nm, Al I at 309.28 nm, Mg I at 285.21 nm, ionized Ca at 315.88 nm, and 317.96 nm. The elements in major and minor amounts are identified by observing the wavelength of the spectral line and labeling that line with the help of the NIST database. The wavelengths are in nanometers, plotted along the x-axis and the intensities along the y-axis.

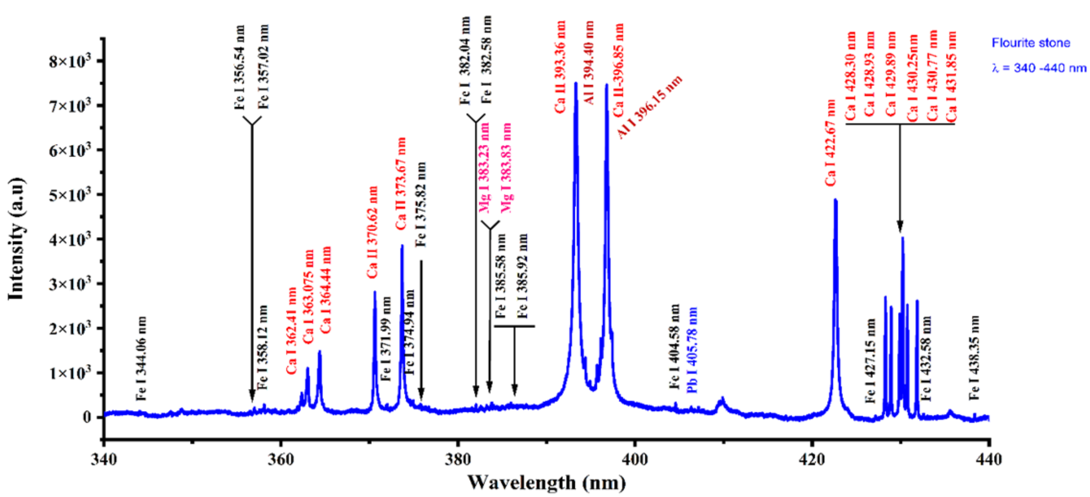

Figure 3. Optical Emission Spectrum of the Fluorite sample representing the spectral line of all the identified elements exists in the range of 340 nm - 440 nm.

In Fig. 3, the highest peak of neutral calcium is observed at 422.65 nm, and the ionized line of 393.96 nm, and Aluminum 394.40 nm are found in the atomic spectrum. The spectral lines of magnesium, for both neutral and ionized lines, iron, and lead are also found with other trace spectra. This spectrum has a wavelength range cover is 340 nm - 440 nm.

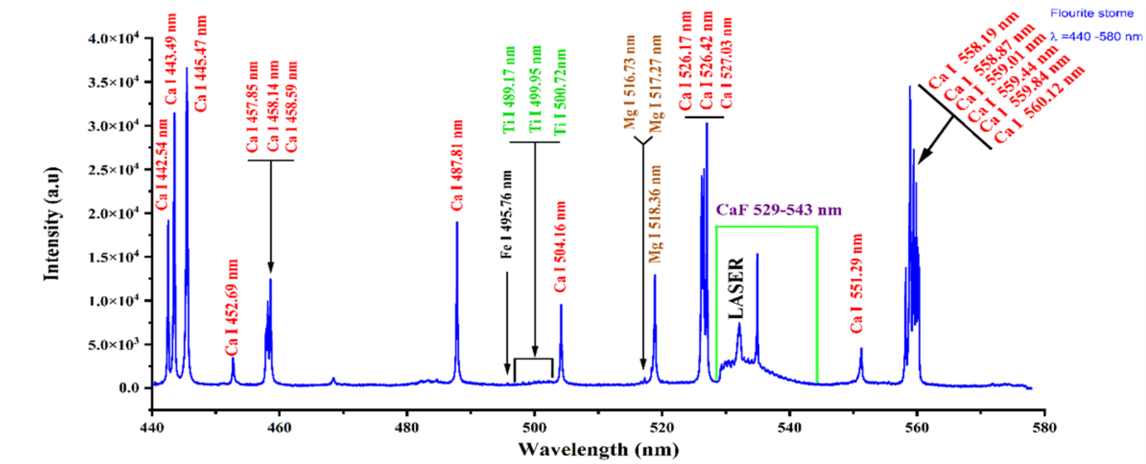

Figure 4. The optical emission spectrum of a fluorite sample representing the spectral line of all the identified elements exists in the range of 440 – 580 nm.

The spectral lines of magnesium, neutral and ionized, and iron line with CaF molecules (range 529 to 543nm) are also detected within the range of 440-580 nm. In Fig. 4 highest peaks of neutral calcium are observed at 445.47 and 588.19nm, and magnesium at 518.36nm are detected in the spectrum.

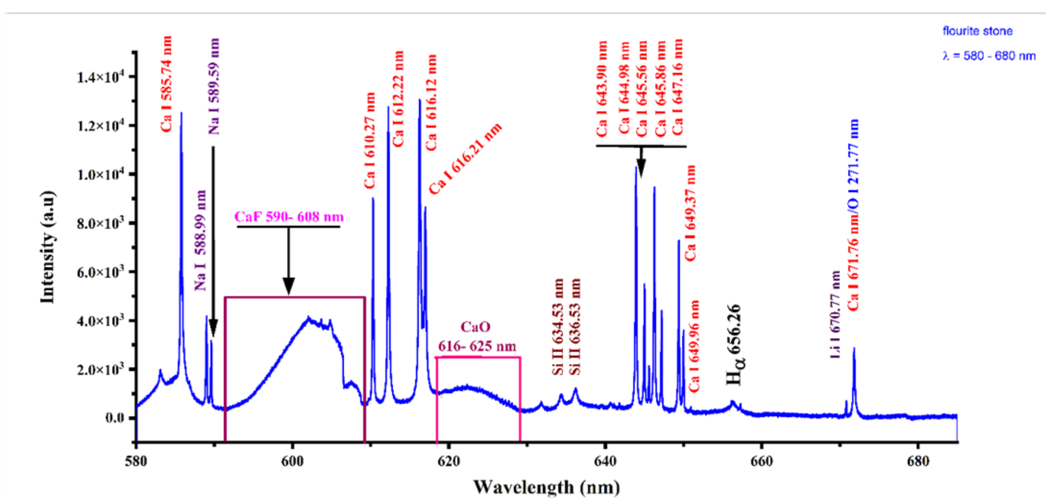

Figure 5. The optical emission spectrum of a fluorite sample representing the spectral line of all the identified elements exists in the range of 580 - 680 nm.

The highest peak of neutral calcium is observed at 585.74 nm, lithium at 760.77 nm, and sodium at 588.99 nm. are observed spectra line shows CaF found at a range of 590 nm- 608 nm, and CaO is at 616 nm – 625 nm. Both molecular spectral lines are also found in the article named “Optimization of fast quantification of fluorine content using handheld LIBS” available at https://www.sciencedirect.com/science/article/pii/S0584854719300527, [5]. They studied the LIBS emission spectrum of a randomly analyzed sample spectral domain ranging from 520 nm to 640 nm that contained the Ca I atomic lines, the CaO, and the CaF molecular bands are those used for the spectral ranges and their baselines in the calibration of the fluorine content (Foucaud et al., 2019, and Cicutto et al., 2016).

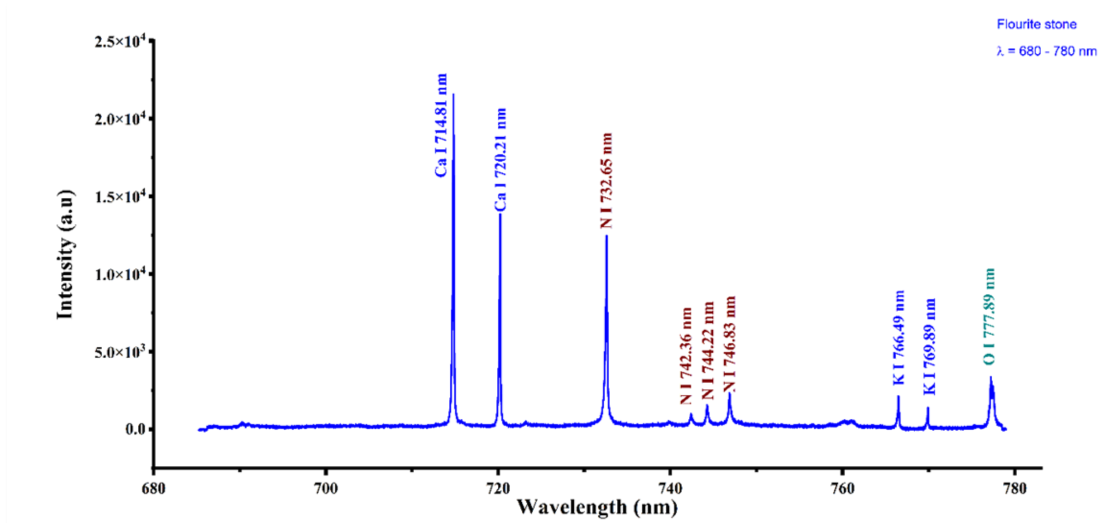

Figure 6. Optical emission spectrum of a fluorite sample representing the spectral line of all the identified elements exists in the range of 680 nm – 780 nm.

The highest peak of neutral calcium is observed at 714.81 nm, and nitrogen at 732.65 nm.

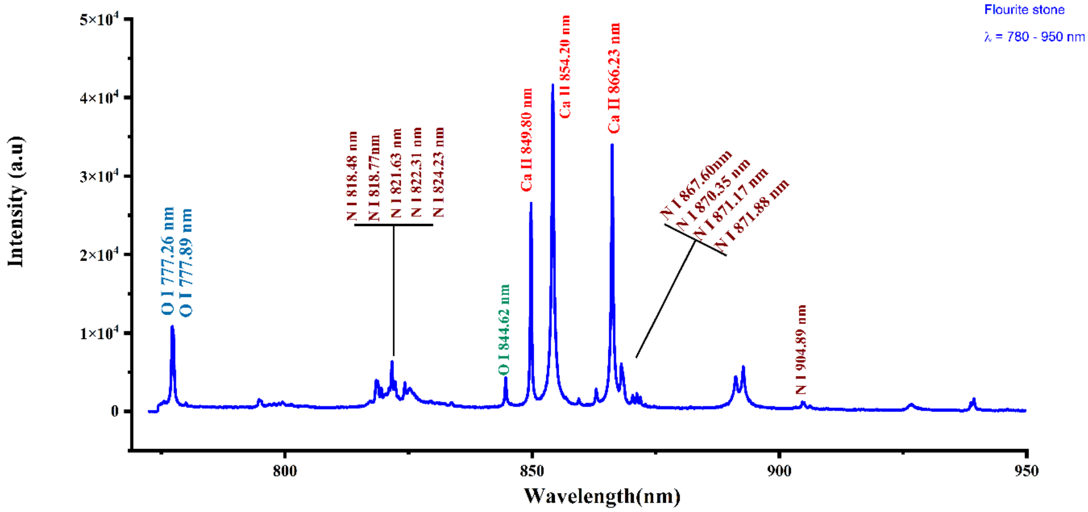

Figure 7. Optical emission spectrum of a fluorite sample representing the spectral line of all the identified elements exists in the range of 780 nm – 950 nm.

In Fig. 07, lines consist of oxygen and nitrogen neutral lines as well as ionized spectral lines, all are in a gas state detected in this range.

4.1 Temperature of Plasma

Now all the required data are available to determine the temperature of the plasma. The Boltzmann plot method is suitable for the calculation of plasma temperature. The distinct spectral lines of Ca-I are selected to find plasma temperature because there is a richness of neutral lines of calcium in the samples. Take all the parameters needed from the NIST database, according to the equation.

$$\ln\left(\frac{\lambda_k I}{g_{k} A_k}\right) = -\frac{E_k}{k_b T} + \ln\left(\frac{FC^s}{U(T)}\right)$$

The plasma temperature is determined from the slope of the straight line and by inverting it. This equation compares with the line equation written as $m \; -\frac{1}{k_b T}$ for the determination of plasma temperature; spectroscopic constants were noted from the NIST database. The first condition is to select spectral lines that are totally free from self-absorption. Suitable neutral lines Ca-I, putting the values in the Saha-Boltzmann equation, then take the inverse to get slope(m) and inverse the value of m ' to determine the electron temperature in Table 02.

The calculated plasma temperature for each sample depends upon the parameters of the sample, and spectroscopic constants are noted from the NIST database. The following figures represent the Saha-Boltzmann plots linearly fit to the origin for different gem samples.

Table 01. Spectroscopic Parameters for all three samples used in drawing Boltzmann Plots.

λ(nm)	**Upper ⟶ Lower**	**Transition Probability×($10^7 ms^{-1}$)**	**G_k**	**E_k (eV)**
429.89	4s4p ⟶ 3p4s	4.66	3	4.76
445.48	4s4p ⟶ 4s4d	8.7	7	4.68
558.88	3d4s ⟶ 3d4p	4.9	7	4.47
559.45	3d4s ⟶ 3d4p	4.8	5	4.73
585.74	3d4p ⟶ 4p	6.6	5	5.04
612.28	4s4p ⟶ 4s5s	2.87	3	3.91
616.21	4s4p ⟶ 4s5s	4.77	3	3.91
643.92	4d4s ⟶ 3d4p	5.3	9	4.45
646.25	4d4s ⟶ 3d4p	4.7	7	4.44

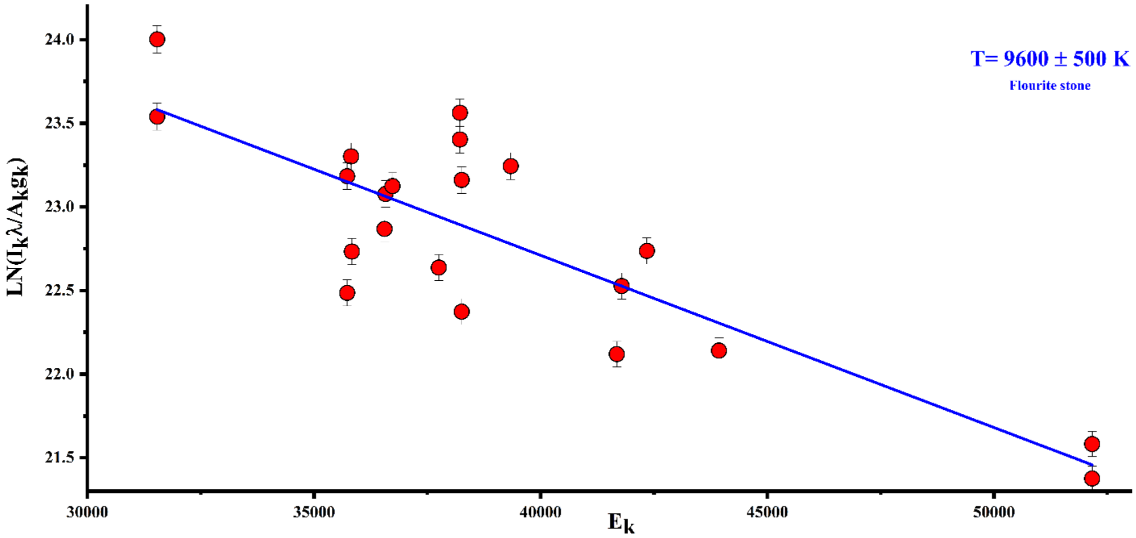

Figure 08. Boltzmann plot for fluorite.

The Boltzmann plots are drawn from samples by using the mentioned constants. The temperature is calculated to be 9600 K, and approximately within a range of 10% is calculated by the formula as:

$$\sigma = \sqrt{\frac{\sum(x_i - u)^2}{N}}$$

The Boltzmann plot for fluorite is represented in Figure 9, clearly showing that the graph fits linearly. Slope of straight-line use for estimation of plasma temperature by the inverse of m=1.290×10^{-4}. The estimated result of the slope calculated temperature of plasma, which is 9600 ± 500 K (0.82 eV), with uncertainty ± 5 %.

4.2 Electron Number Density (Ne)

Electron number density can be estimated by using any spectral line free from self-absorption. The most common method used to estimate electron number density is Stark broadening, and its neutral or ionized line is used to calculate Ne.

$$N_e = (\frac{\Delta\lambda_{FWHM}}{2\omega_s})1.47^{\times}10^{17}$$

Table 03. Electron Number Density for a Fluorite Sample of Gem Sample.

Samples	Coefficient	ΔE^3	$\Delta T^{1/2}$	$Ne \geq 1.4 \times e^{12}\, Te^{1/2}(\Delta E^3)\ cm^{-3}$
Fluorite	1.4×10^{12}	8.36	97.97	3.1×10^{15}

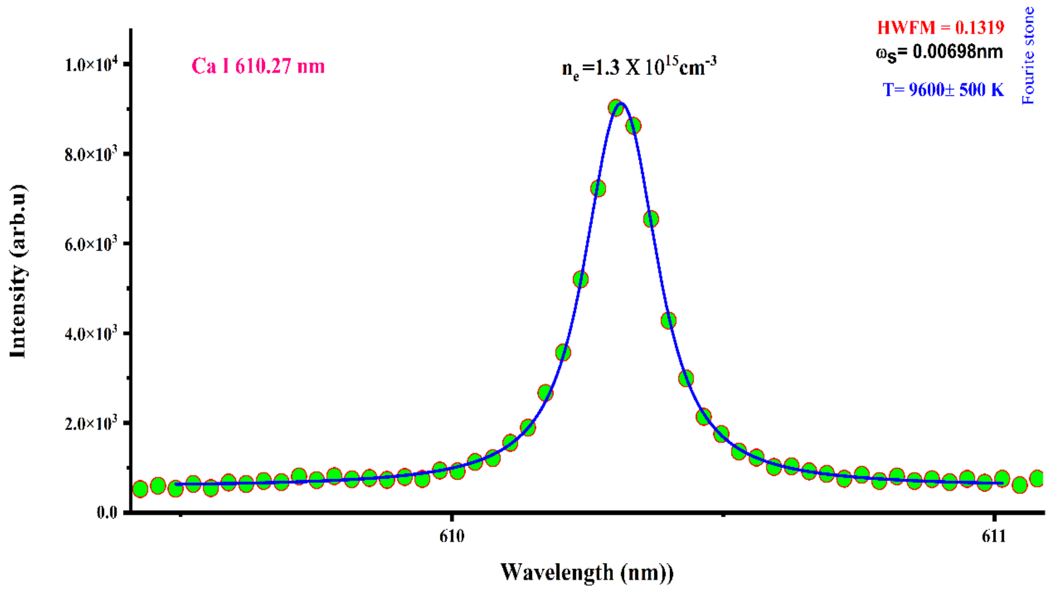

Figure 09. Stark broadened line of Ca I fitted with a Voigt function for fluorite.

By broadening constant ω_s = 0.00698 nm, Al-I at 309.89 nm, which is optically thin for estimating electron number density, which is 8.34×10^{16} cm^{-3}. The line profile is observed experimentally, dots, and fitted Voigt function shown in fig.10, and the calculated value is given in Table 04.

Table 04. McWhirter's standard for Fluorite.

Sample	Element	ω (nm)	$\Delta\lambda_{FWHM}$
Fluorite	Ca	6.69×10^{-3}	3.1×10^{15}

4.3 Optically Thin Condition

Optically thin condition of fluorite by CF-LIBS is determined by considering an equation given as:

$$\frac{I_{ki}}{I_{nm}} = \frac{A_{ki}\ g_k\ \lambda_{nm}}{Anm\ g_{n\,\lambda_{ki}}} \exp\left(\frac{|E_k - E_n|}{k_{b\,T}}\right)$$

Selected two spectral lines and found values of these quantities from the NIST site, where ki and nm. A_{ki}, $I_{ki,}$ and λ_{ki} are the transition probability, intensity, and wavelength of the first line. Where g_k is the weight of transformation from k to I, g_{nm} is the weight of transformation from n to m, T is the temperature of plasma, and K_b represents the Boltzmann constant.

In the above equitation's the intensity ratio on the right side while their result must be equal to the same side. To check the optically thin condition of plasma, neutral lines of calcium are taken. It can be clearly seen from the results in Table 05.

Table 5. Optically Think Condition for Fluorite gem samples.

Sample	**Element**	**λ (nm)**	**A_k**	**g_k**	**ΔE(eV)**	**Expt:$\frac{I1}{I2}$**	**Theoretical $\frac{I1}{I2}$**	**error**
Fluorite	Ca	428.30	6.0×10^7	3	0.82	1.07	1.03	3.8 %
		429.88	4.7×10^7	3	0.82			

4.4 Concentration of fluorite gemstones Using CF-LIBS

The neutral elements present in Fluoride can be calculated as

$$FC^z = \frac{U^z(T)\ I_k}{g_k A_k}\ e^{\frac{E_k}{TK_B}}$$

The ionized elements found in fluorite gemstones are calculated

$$n_e \frac{C^{z+1}}{C^z} = \frac{(2Tm_e\ K_B)^{\frac{3}{2}}}{h^3}\ \frac{2U_{z+1}}{U_z} \text{Exp}\left[-\ \frac{E_{ion}}{TK_B}\right] \text{cm}^{-3}$$

Total concentration of neutral and ionized elements present in fluorite stones.

$$C_T = C_Z + C_{Z+1}$$

The Weight percentage is calculated by the formula:

$$\text{CelementC} \times 100\%$$

The calculated concentrations of all different elements in Fluorite are given in Table 06.

Table 06 Concentration of Elements Present in fluorite.

Element	Ca	Si	Mg	Fe	Na	Li	Al	K	Ti	Total Wt%
Fluorite Wt %	87.89	0.88	1.28	8.92	0.066	0.004	0.47	0.124	0.35	100

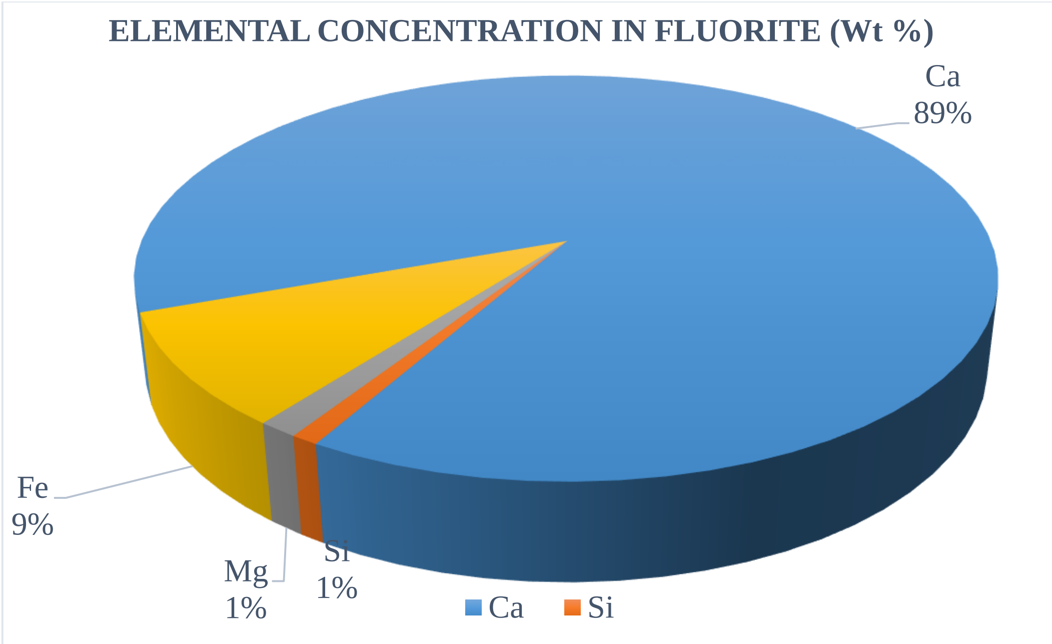

Figure 10. Pi chart of Fluorite's elemental compositions.

5. Discussion

Fluorite gemstones have unique compositions compared to other natural rocks. Based on which it's adorable, attractive, multi-colors, different hardnesses, and preciousness. The unique molecular structure of CaF and CaO found in fluorite, with patterns as shown in Figs. 04 & 05 are the same as Foucaud et al. in 2019 [5]. Different Emission spectral lines of Ca-I lines at 315.88 nm, 317.93 nm, 428.30 nm, 430.24 nm, 442.54 nm, 445.45 nm, 527.05 nm, 551.56 nm, 560.56 nm, 610.27 nm, 612.22 nm, and 616.27 nm are used to measure the concentration of Ca. The concentration of Si-I is calculated by using emission lines of 250.68, 251.61, 263.12, and 288.16 nm. For the concentration of Na-I, the 588.99 nm and 589.59 nm emission lines are used. And for Li-I, 760.77 nm, for Al-I, 393.40 nm, and 396.15 nm emission lines are used. There are found bands of CaF and CaO [27], and a small amount of Si, Al, and Mg are reported as impurities of extremely variable colors: colorless, white, yellow, green, blue, and purple, etc. The concentration of elements in percentage weight found in fluorite is 88 % Ca, 9% Fe, 1 % Al, 1% Si, and 1 % Mg as given in Fig. 10.

6. Conclusion

Unique concentration of various elements is shown in Table 6, where the secret preciousness of fluorite gemstone is compared to other natural stone molecular states of CaF and CaO. Gilgit-

Baltistan is one of the base camps of at least all kinds of precious stones are found. Fluorite gemstones are distinguished from other gemstones and rocks because the CaF & CaO are detected by a comparative study of the emission spectral line of Article Optimization of fast quantification of fluorine content using handheld LIB has found a similar graph. The major concentration is (88 %) Ca element in weight percentage found in fluorite, the remaining 12% is the minor elements.

Acknowledgement:

We are thankful to the National Center for Physics, Islamabad, for their cooperation and facilitation during our study.

Funding Statement:

This is totally academic research, and no funds were taken for this study.

Conflict of Interest:

There is no conflict of interest among authors.

Data Availability:

All data are available and can be shared for research purposes.

Author's Contribution:

Muhammad Raza idealized the whole study and wrote the whole article in its present format, and Muhammad Sharief carried out the practical work and analyzed the data.

References:

[1]. Fahad, M., Farooq, Z., & Abrar, M. Comparative study of calibration-free laser-induced breakdown spectroscopy methods for quantitative elemental analysis of quartz-bearing limestone. Applied Optics, 58(13), 3501, (2019).

[2]. Godwal, Y., Taschuk, M. T., Lui, S. L., Tsui, Y. Y., Fedosejevs, R., & Tg, C. Laser-Induced Breakdown Spectroscopy for Microanalysis. 3rd International Conference on the Frontiers of Plasma Physics and Technology, 1–10, (2008).

[3]. Abbasi, S. A., Rafique, M., Mir, A. A., Kearfott, K. J., Ud-Din Khan, S., Ud-Din Khan, S., Khan, T. M., & Iqbal, J. Quantification of elemental composition of Granite Gneiss collected from Neelum Valley using calibration-free laser-induced breakdown and energy-dispersive X-ray spectroscopy. Journal of Radiation Research and Applied Sciences, 13(1), 362–372, (2020).

[4]. Fortes, F. J., Moros, J., Lucena, P., Cabalín, L. M., & Laserna, J. J. Laser-induced breakdown spectroscopy. Analytical Chemistry, 85(2), 640–669, (2013).

[5]. Foucaud, Y., Fabre, C., Demeusy, B., Filippova, I. V., & Filippov, L. O. Optimization of fast quantification of fluorine content using handheld LIBS. 1–36, (2019).

[6]. Senesi, G. S., Manzini, D., & De Pascale, O. Application of a laser-induced breakdown

spectroscopy handheld instrument to the diagnostic analysis of stone monuments. Applied Geochemistry, 96(June), 87–91, (2018).

[7]. Koral, C., Dell'Aglio, M., Gaudiuso, R., Alrifai, R., Torelli, M., & De Giacomo, A. Nanoparticle-Enhanced Laser Induced Breakdown Spectroscopy for the noninvasive analysis of transparent samples and gemstones. Talanta, 182(December 2017), 253–258, (2018).

[8]. Hu, Z., Zhang, D., Wang, W., Chen, F., Xu, Y., Nie, J., Chu, Y., & Guo, L. A review of calibration-free laser-induced breakdown spectroscopy. TrAC - Trends in Analytical Chemistry, 152, 116618, (2022).

[9]. Krishnan, S., & Mudrich, M. Intense laser matter interaction in atoms, finite systems and condensed media: recent experiments and theoretical advances. European Physical Journal: Special Topics, 230(23), 3981–3988, (2021).

[10]. Singh, V. K., Kumar, V., & Sharma, J. Importance of laser-induced breakdown spectroscopy for hard tissues (bone, teeth) and other calcified tissue materials. Lasers in Medical Science, 30(6), 1763–1778, (2015).

[11]. Ahmed, R., Akthar, M., Jabbar, A., Umar, Z. A., Ahmed, N., Iqbal, J., & Baig, M. A. Signal Intensity Enhancement by Cavity Confinement of Laser-Produced Plasma. IEEE Transactions on Plasma Science, 47(3), 1616–1620, (2019).

[12]. Abbass, Q., Ahmed, N., Ahmed, R., & Baig, M. A. A Comparative Study of Calibration Free Methods for the Elemental Analysis by Laser Induced Breakdown Spectroscopy. Plasma Chemistry and Plasma Processing, 36(5), 1287–1299, (2016).

[13]. Singh, V. K., Rai, A. K., Rai, P. K., & Jindal, P. K. Cross-sectional study of kidney stones by laser-induced breakdown spectroscopy. Lasers in Medical Science, 24(5), 749–759, (2009).

[14]. Winefordner, J. D., Gornushkin, I. B., Correll, T., Gibb, E., Smith, B. W., & Omenetto, N. Comparing several atomic spectrometric methods to the super stars: Special emphasis on laser induced breakdown spectrometry, LIBS, a future super star. Journal of Analytical Atomic Spectrometry, 19(9), 1061–1083, (2004).

[15]. Ruas, A., Matsumoto, A., Ohba, H., Akaoka, K., & Wakaida, I. Application of laser-induced breakdown spectroscopy to zirconium in aqueous solution. Spectrochimica Acta - Part B Atomic Spectroscopy, 131, 99–106, (2017).

[16]. Kim, H., Jeon, Y., Lee, W. B., Nam, S. H., Han, S. H., Ham, K. S., Singh, V. K., & Lee, Y. Feasibility of Quantitative Analysis of Magnesium and Calcium in Edible Salts Using a Simple Laser-Induced Breakdown Spectroscopy Device. Applied Spectroscopy, 73(10), 1172–1182, (2019).

[17]. Agheem, M. H., Shah, M. T., Khan, T., Murata, M., Arif, M., & Dars, H. Shigar Valley gemstones, their chemical composition and origin, Skardu, Gilgit-Baltistan, Pakistan. Arabian Journal of Geosciences, 7(9), 3801–3814, (2014).

[18]. Fayyaz, A., Asghar, H., & Alrebdi, T. A. Results in Physics Laser-Induced breakdown spectroscopy and Energy-Dispersive X-ray analyses for green mineral fluorite (CaF 2).

Results in Physics, 52(May), 106850, (2023).
[19]. Martin, J. E. Physics for Radiation Protection, A Handbook, Second Edition, Completely Revised and Enlarged, (2008).
[20]. Lasmanis, R. Green Fluorite from the Kettle Mine, Ferry County, Washington. Rocks & Minerals, 76(4), 218–221, (2001).
[21]. Almeida, C. S. de, Miccoli, L. S., Andhini, N. F., Aranha, S., Oliveira, L. C. de, Artigo, C. E., Em, A. A. R., Em, A. A. R., Bachman, L., Chick, K., Curtis, D., Peirce, B. N., Askey, D., Rubin, J., Egnatoff, D. W. J., Uhl Chamot, A., El-Dinary, P. B., Scott, J.; Marshall, G., Prensky, M., … Santa, U. F. De. Metode Penelitian Kuantatif. In Revista Brasileira de Linguística Aplicada, 5(1), (2016).
[22]. Aigbe, S. O., Ewa, I. O. B., Ogunleye, P. O., & Oladipo, M. O. A. Elemental characterization of some Nigerian gemstones: Tourmaline, fluorite, and topaz by instrumental neutron activation analysis. Journal of Radioanalytical and Nuclear Chemistry, 295(1), 801–805, (2013).
[23]. Sharif, M., Raza, M., & Umer, Z. A. Elemental Analysis of Black Tourmaline Found in the Mines of Astak Valley, Gilgit-Baltistan (GB), by Using Calibration Free Laser Induced Breakdown Spectroscopy (CF-LIBS). Xi'an Shiyou Daxue Xuebao (Ziran Kexue Ban)/Journal of Xi'an Shiyou University, Natural Sciences Edition, 18(10), (2022).
[24]. Martinez, M., Harry, G. J., Haynes, E. N., Lin, P. D., Oken, E., Horton, M. K., Wright, R. O., Arora, M., & Austin, C. Quantitative fluoride imaging of teeth using CaF emission by laser induced breakdown spectroscopy. Journal of Analytical Atomic Spectrometry, 38(2), (2023).
[25]. Shakeel, H., Haq, S. U., Aisha, G., & Nadeem, A. Quantitative analysis of Al-Si alloy using calibration free laser induced breakdown spectroscopy (CF-LIBS). Physics of Plasmas, 24(6), (2017).
[26]. Hedwig, R., Lie, Z. S., Kurniawan, D. P., Kurniawan, K. H., Lie, T. J., & Idris, N. Evidence of feasible hardness test on Mars using ratio of ionic / neutral emission intensities measured with laser-induced breakdown spectroscopy in low pressure CO2 ambient gas. Journal of Applied Physics, 119(16), (2016).
[27]. Álvarez, C., Pisonero, J., & Bordel, N. Quantification of fluorite mass-content in powdered ores using a Laser-Induced Breakdown Spectroscopy method based on the detection of minor elements and CaF molecular bands. Spectrochimica Acta - Part B Atomic Spectroscopy, 100, 123–128, (2014).